Controlling Exciton-Phonon Interactions via Electromagnetically Induced Transparency

V. Walther,[1,2,*,†] P. Grünwald,[2,†] and T. Pohl[2]
[1]ITAMP, Harvard-Smithsonian Center for Astrophysics, Cambridge, Massachusetts 02138, USA
[2]Center for Complex Quantum Systems, Department of Physics and Astronomy, Aarhus University, Ny Munkegade 120, 8000 Aarhus C, Denmark

(Received 9 July 2020; accepted 25 September 2020; published 20 October 2020)

Highly excited Rydberg states of excitons in Cu_2O semiconductors provide a promising approach to explore and control strong particle interactions in a solid-state environment. A major obstacle has been the substantial absorption background that stems from exciton-phonon coupling and lies under the Rydberg excitation spectrum, weakening the effects of exciton interactions. Here, we demonstrate that two-photon excitation of Rydberg excitons under conditions of electromagnetically induced transparency (EIT) can be used to control this background. Based on a microscopic theory that describes the known single-photon absorption spectrum, we analyze the conditions under which two-photon EIT permits separating the optical Rydberg excitation from the phonon-induced absorption background, and even suppressing it entir7ely. Our findings thereby pave the way for the exploitation of Rydberg blockade with Cu_2O excitons in nonlinear optics and other applications.

DOI: 10.1103/PhysRevLett.125.173601

The ability to control and manipulate highly excited Rydberg states of atoms has led to numerous breakthroughs, from simulating quantum magnetism [1–8] and performing quantum gates [9–11], to quantum and nonlinear optics [12–21].

In 2014, it was demonstrated that semiconductor excitons in bulk Cu_2O crystals can also be excited to Rydberg states, which can be as large as their atomic counterparts [22]. Their enormous size implies a high susceptibility to magnetic [23–29] and electric [30–33] fields, that may be exploited in integrated semiconductor microstructures [34,35]. Importantly, the resulting long-range interactions of such large excitons [36], combined with the characteristic hydrogenlike scaling of the energy levels and lifetimes [37], can give rise to a strong suppression of Rydberg excitation, high optical nonlinearities [38,39], and topological states [40]. A key prerequisite for exploiting such interaction effects in future experiments and potential applications is the availability of isolated Rydberg excitation lines. While this is excellently satisfied in atomic systems, the observed excitonic Rydberg series in Cu_2O rests on a broad background that accounts for more than 50% of the optical density on some Rydberg-state resonance. Stemming from the simultaneous excitation of an optical phonon and a deeply bound exciton [41,42], this background represents an additional excitation channel that inevitably competes with the Rydberg-exciton series. Since such a competition naturally weakens many effects of excited-state interactions, controlling the phonon-induced absorption background and resonant Rydberg-state excitation remains an important challenge.

In this Letter, we demonstrate that this can be achieved via electromagnetically induced transparency (EIT) [43,44] involving excited exciton states. Two-photon excitation of long-lived excitons in s states via a low-lying p state [45,46] [see Fig. 1(a)], hereby leads to interference of the two excitation pathways that can be used to eliminate the population of the strongly coupled and rapidly decaying

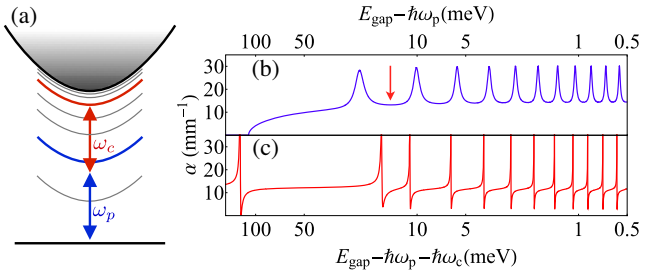

FIG. 1. EIT in Cu_2O. (a) A weak probe laser with a frequency ω_p generates p-state excitons of the yellow series. The simultaneous coupling to a continuum of phonon-dressed exciton states gives rise to the typical absorption spectrum of Cu_2O below the band gap energy E_{gap} of the yellow series, as shown in (b). As further illustrated in panel (a), an additional control laser field with a frequency ω_c couples the generated excitons to an excited s state of the yellow series to establish conditions of electromagnetically induced transparency. As shown in panel (c), this makes it possible to control the spectroscopic properties of the material and leads to a series of narrow absorption dips at a given s-state resonance with a greatly suppressed absorption background at each minimum. The depicted spectrum is scanned by varying ω_c with a fixed ω_p as indicated by the red arrow in panel (b).

intermediate state. Here, we show that this effect cannot only be employed to achieve narrow Rydberg-exciton lines but also allows us to control and even reduce the broad phonon background that would otherwise supplement the exciton spectrum [see Figs. 1(b), 1(c)]. Depending on the material parameters, we identify three distinct regimes in which either the discrete exciton lines or the broad phonon background are suppressed individually, or where both vanish simultaneously to yield transparency on two-photon resonance. The results of this work, thereby, suggest novel experimental probes of optical processes and phonon effects in semiconductors, and open the door to nonlinear optics and explorations of many-body phenomena with interacting Rydberg excitons.

Cuprous oxide features four exciton series, the yellow, green, blue, and violet series, which couple to light in the respective optical frequency domains. Most spectroscopic studies of Cu_2O are based on the excitation of p-state excitons of the yellow series, with wavelengths of ~590 nm [47–51]. Around each resonance, the light field couples to a p-state exciton that can be described by a bosonic field operator $\hat{X}_p$, and is excited with a linewidth Γ_p, an exciton-photon coupling strength g_p [41] and a frequency detuning $\hbar\delta_p = E_p - \hbar\omega_p$, defined by the exciton energy E_p and laser frequency ω_p. However, early measurements of the series [22] have established the presence of a broad absorption background that starts above the energy E_0 of the $1s$-ortho exciton and extends all the way across the band edge [Fig. 1(b)]. In the underlying absorption process, a photon virtually excites an intermediate state, which subsequently decays into an optical phonon and a $1s$-ortho exciton [41]. This indirect excitation process is necessary since neither the generation of the phonon nor the excitation of the $1s$ exciton is dipole allowed. The dominant involved intermediate states have recently been identified as the s states from the blue exciton series, mentioned above. Among the multitude of phonon modes in Cu_2O, the optical phonons with Γ_3^- symmetry make the single most important contribution to the decay process [42].

The underlying exciton-phonon scattering process can be well described by a Fröhlich interaction term

$$\hat{H}_F = \sum_\mu \int d^3q d^3q' h_\mu(\mathbf{q},\mathbf{q}') \times [\hat{b}^\dagger(-\mathbf{q})\hat{X}_{1s}^\dagger(\mathbf{q}+\mathbf{q}')\hat{X}_\mu(\mathbf{q}') + \text{H.c.}], \quad (1)$$

where low-lying excitons from the blue series at momentum $\mathbf{q}'$, described by the operator by $\hat{X}_\mu(\mathbf{q}')$, decay into a pair of a $1s$-exciton at momentum $\mathbf{q}+\mathbf{q}'$, described by $\hat{X}_{1s}(\mathbf{q}+\mathbf{q}')$, and a phonon that carries the excess momentum and is described by the bosonic operator $\hat{b}(-\mathbf{q})$. The rate of this process is determined by the coupling constant $h_\mu(\mathbf{q},\mathbf{q}')$. While the kinetic energy of the $1s$-exciton of mass m and rest energy E_0 leads to a momentum-dependent detuning $\hbar\delta_0(\mathbf{q}) = E_0 + \hbar^2q^2/(2m) - \hbar\omega_p$, the phonon dispersion, $\hbar\omega_{\Gamma_3^-}$, can be taken as constant across the relevant phonon momenta. The blue exciton states are far off-resonant ($|\delta_\mu| \approx 0.4$ eV) and therefore only weakly populated. One can, thus, apply adiabatic elimination of their fast dynamics to describe the overall scattering process in terms of the composite bosons $\hat{X}(\mathbf{q},\mathbf{q}') = \hat{b}(-\mathbf{q})\hat{X}_{1s}(\mathbf{q}+\mathbf{q}')$ [52], with a complex linewidth $\gamma(\mathbf{q},\mathbf{q}') = \Gamma + i[\delta_0(\mathbf{q}+\mathbf{q}') + \omega_{\Gamma_3^-}]$ and effective optical coupling elements

$$g(\mathbf{q},\mathbf{q}') = \sum_\mu g_\mu/\delta_\mu \cdot h_\mu(\mathbf{q},\mathbf{q}'). \quad (2)$$

It is this optical coupling to the associated continuum of states that leads to the broad absorption background described above.

As we will show below, however, EIT can be used to control the phonon coupling through the formation of an excitonic dark state. Establishing EIT requires a third state that is relatively stable and can be excited via a two-photon process (Fig. 2). A natural choice is a Rydberg s-state, which we describe by the operator $\hat{X}_s$. Hereby, another laser field with a frequency ω_c couples the generated p-state excitons to the long-lived Rydberg s state with Rabi frequency Ω_s and frequency detuning $\hbar\delta_s = E_s - \hbar\omega_p - \hbar\omega_c$. The resulting three-level system features a dark state of the form $\sim -g_p/\Omega_s\hat{X}_s^\dagger|0\rangle$.

In addition, however, the control field laser also couples to the continuum states since $\hat{X}_p$ and $\hat{X}$ share the same parity. The associated Rabi frequency can be obtained by

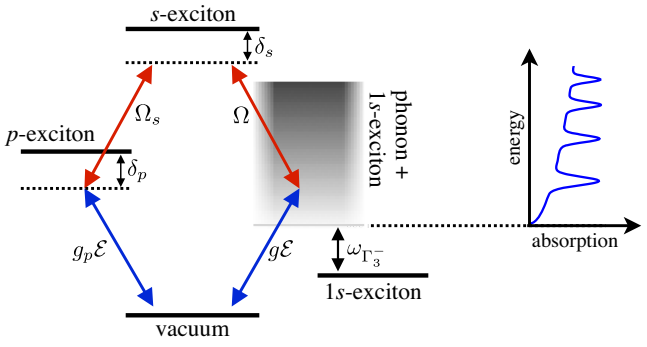

FIG. 2. The incident probe laser with electric field amplitude $\mathcal{E}$ excites p-state excitons with an optical coupling strength g_p and detuning δ_p. Simultaneously, the field couples to the continuum of phonon-dressed $1s$ excitons with coupling strength g. The dressed states start to appear at an energy $\hbar\omega_{\Gamma_3^-}$ above the $1s$ state. The combination of the p-state excitation and the phonon-dressed excitons generate the broad absorption spectrum sketched on the right [cf. Fig. 1(b)]. As we show in this Letter, this typical absorption can be controlled by a second light field that couples both types of excitons to an s state with coupling strengths Ω_s and Ω, respectively, and a two-photon detuning δ_s.

adiabatically eliminating the dynamics of the blue intermediate states as before yielding $\Omega(\mathbf{q},\mathbf{q}') = \sum_\mu \Omega_\mu/\delta_\mu \cdot h_\mu(\mathbf{q},\mathbf{q}')$. Like the isolated Rydberg states, the background alone can also establish an EIT dark state that carries no contribution from the intermediate states and is of the form $\sim -D_{g\Omega}/D_{\Omega^2}\hat{X}_s^\dagger|0\rangle$ with

$$D_{\Omega^2} = \int d^3q \frac{\Omega^2(\mathbf{q},\mathbf{q}')}{\gamma(\mathbf{q},\mathbf{q}')},$$
$$D_{g\Omega} = \int d^3q \frac{g(\mathbf{q},\mathbf{q}')\Omega(\mathbf{q},\mathbf{q}')}{\gamma(\mathbf{q},\mathbf{q}')}. \tag{3}$$

Taken separately, the two excitation pathways, shown in Fig. 2, therefore promote the formation of simple dark states with vanishing absorption on two-photon resonance. Their simultaneous presence, however, leads to a competition between each pathway that can be described by the following set of Heisenberg equations for the exciton operators

$$\dot{\hat{X}}_p(\mathbf{q}) = -\gamma_p \hat{X}_p(\mathbf{q}) - ig_p\mathcal{E}(\mathbf{q}) - i\Omega_s\hat{X}_s(\mathbf{q}), \tag{4}$$

$$\dot{\hat{X}}_s(\mathbf{q}) = -\gamma_s \hat{X}_s(\mathbf{q}) - i\Omega_s\hat{X}_p(\mathbf{q}) + i\int d^3q'\Omega(\mathbf{q}',\mathbf{q})\hat{X}(\mathbf{q}',\mathbf{q}) \tag{5}$$

$$\dot{\hat{X}}(\mathbf{q},\mathbf{q}') = -\gamma(\mathbf{q},\mathbf{q}')\hat{X}(\mathbf{q},\mathbf{q}') + ig(\mathbf{q},\mathbf{q}')\mathcal{E}(\mathbf{q}') + i\Omega(\mathbf{q},\mathbf{q}')\hat{X}_s(\mathbf{q}'), \tag{6}$$

where we have defined $\gamma_{p/s} = \Gamma_{p/s} + i\delta_{p/s}$, and $\mathcal{E}$ denotes the amplitude of the probe-light field. Note that a generalization to multiple exciton states is straightforward [see Fig. 1(b)], and only leads to small interference effects for overlapping resonances [53].

These equations are readily solved for the steady-state expectation values, which yield the susceptibility

$$\chi^{(1)}(\mathbf{q})\mathcal{E}(\mathbf{q}) = -\frac{g_p}{cn}\langle\hat{X}_p(\mathbf{q})\rangle + \int d^3q' \frac{g(\mathbf{q}',\mathbf{q})}{cn}\langle\hat{X}(\mathbf{q}',\mathbf{q})\rangle, \tag{7}$$

where $n \approx 2.74$ is the refractive index of Cu_2O. The first term on the right-hand side describes the coherence of the discrete p-state exciton, while the second term captures the contribution of the phonon-induced absorption background. The susceptibility in Eq. (7) describes the linear optical response, which is valid at sufficiently low probe-field intensities, below the onset of nonlinearities mediated by the strong Rydberg interactions [32,38]. The inverse absorption length in the crystal is then given by $\alpha = \mathrm{Im}(\chi^{(1)})$. Explicitly, we find from Eqs. (4)–(7) [52]

$$i\chi^{(1)} = \frac{g_p}{cn}\frac{\Omega_s D_{g\Omega} - g_p(\gamma_s + D_{\Omega^2})}{\gamma_p(\gamma_s + D_{\Omega^2}) + \Omega_s^2} - \frac{D_{g^2}}{cn} + \frac{D_{g\Omega}}{cn}\frac{D_{g\Omega}\gamma_p + g_p\Omega_s}{\gamma_p(\gamma_s + D_{\Omega^2}) + \Omega_s^2}, \tag{8}$$

with the additional parameter

$$D_{g^2} = \int d^3q' \frac{g^2(\mathbf{q}',\mathbf{q})}{\gamma(\mathbf{q}',\mathbf{q}')}. \tag{9}$$

Without the coupling laser, the absorption is simply given by the sum of the yellow exciton and the background, $icn\chi^{(1)} = -g_p^2/\gamma_p - D_{g^2}$ [42]. The observed characteristic square-root behavior of the latter [54] is recovered if we assume metastable continuum states ($\Gamma = 0$ [52]) and use a constant interaction coefficient over the range of relevant momenta, $h_\mu(\mathbf{q},\mathbf{q}') = \text{const}$. In this case, the two optical coupling elements are constant, $g(\mathbf{q},\mathbf{q}') = g$ and $\Omega(\mathbf{q},\mathbf{q}') = \Omega$. Denoting the maximal kinetic energy of the $1s$ exciton as $\bar{E}$, Eq. (9) can be integrated straightforwardly across the entire Brillouin zone yielding

$$D_{g^2} = \frac{8\pi^2 g^2 m^{3/2}}{\sqrt{2}\hbar^2}\left(\sqrt{\hbar\omega_p - E_0 - \hbar\omega_{\Gamma_3^-}} - i\frac{2}{\pi}\sqrt{\bar{E}}\right) \tag{10}$$

for probe laser energies $\hbar\omega_p \geq E_0 + \hbar\omega_{\Gamma_3^-}$. This simple expression indeed describes the experimentally observed ω_p dependence to a high accuracy [54], justifying the simplification of the exciton phonon coupling, $h_\mu(\mathbf{q},\mathbf{q}') = \text{const}$ This also simplifies the parameters $D_{\Omega^2} = (\Omega^2/g^2)D_{g^2}$ and $D_{g\Omega} = (\Omega/g)D_{g^2}$ and permits reducing the total susceptibility to

$$i\chi^{(1)} = -\frac{\gamma_s(g_p^2 + D_{g^2}\gamma_p) + (g_p\Omega - g\Omega_s)^2(\frac{D_{g^2}}{g^2})}{\gamma_p(\gamma_s + \frac{\Omega^2}{g^2}D_{g^2}) + \Omega_s^2}. \tag{11}$$

Since the Rydberg-state linewidth Γ_s is typically small, the resonant absorption is largely determined by the second term in the numerator, which is controlled by the ratio $\beta = g_p\Omega/(g\Omega_s)$. Note that β does not depend on the control field intensity but represents a material constant.

Figure 3(a) shows the absorption profile for different values of this parameter. If $\beta = 1$, the yellow p states and the phononic background feature identical dark states. Under such conditions of congruent EIT, the two excitation pathways do not perturb each other, such that one can suppress absorption on two-photon resonance. For different values $\beta \neq 1$, the competition between the pathways leads to a finite EIT dip. In the limit of $\beta \ll 1$, excitation via the yellow series is dominant and therefore experiences EIT, allowing the resonant absorption to drop to the background value α_{bg}. In the opposite limit of $\beta \gg 1$, this background

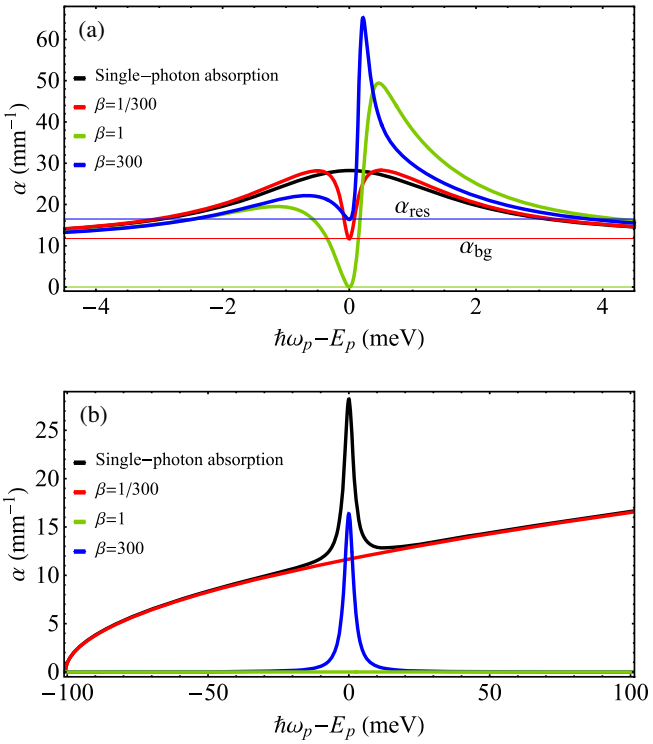

FIG. 3. Probe field absorption spectra around the $2p$ exciton at an energy E_p. In panel (a) the control field is tuned to resonance with the Rydberg-state transition, i.e., $\delta_p = \delta_s$. The parameters of the probe-field transitions are taken from Ref. [42], and the Rydberg decay is neglected, $\Gamma_s = 0$. The different colored curves show typical absorption profiles for different indicated values of $\beta = g_p\Omega/(g\Omega_s)$, whereby the larger of the two Rabi frequencies Ω and Ω_s is chosen to be 0.50 meV. For comparison, the black line shows the absorption spectrum in the absence of EIT, i.e., for $\Omega_s = \Omega = 0$. The thin horizontal lines indicate the resonant probe absorption stemming only from the $2p$ exciton (α_{res}) and only from the background (α_{bg}). Panel (b) shows the same quantities for identical parameters, but with the control field tuned to two-photon resonance, $\delta_s = 0$.

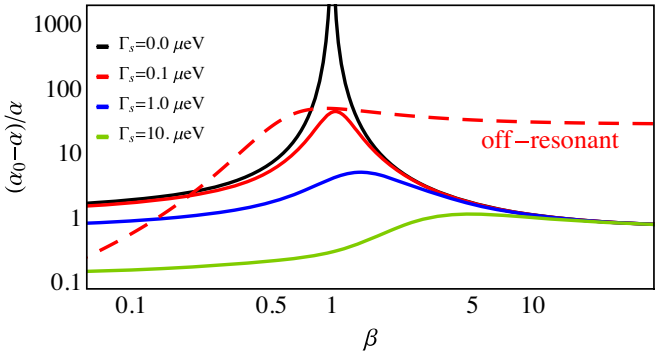

FIG. 4. Absorption contrast as a function of β for different indicated values of Γ_s on $2p$-exciton resonance and two-photon resonance ($\delta_p = \delta_s = 0$). β is varied by changing Ω while $\Omega_s = 50$ μeV is held constant, and the remaining parameters coincide with those of Fig. 3. The dashed line shows the absorption contrast for $\Gamma_s = 0.1$ μeV and probe laser tuned away from the $2p$ resonance at $\delta_p = 20$ meV. β is varied by changing Ω_s with $\Omega = 50$ μeV.

absorption can be suppressed via EIT and the residual absorption is that of the p resonance, α_{res}.

If the control laser is tuned to two-photon resonance, the quantum state stays in the approximate dark state when scanning the p resonance [Fig. 3(b)]. Under conditions of congruent EIT, the system then becomes transparent for all probe detunings. Dominant EIT on the p state excitons ($\beta \ll 1$) leads to an isolated phonon background that extends across the entire yellow series. On the other hand, if the phononic background experiences EIT ($\beta \gg 1$), it is entirely suppressed and one can realize a series of sharp isolated p-state resonances, as indicated by the blue line in Fig. 3(b).

It is interesting to note that the presence of the coupling laser can even increase the probe field absorption [see Fig. 3(a)]. This effect occurs on the blue-detuned side of the resonance and is due to interference of the excitation pathways, where the phonon continuum yields an additional effective decay of the s state.

A key ingredient to leverage the power of Rydberg interactions optically is a large interaction-induced absorption contrast, which would result in a large nonlinearity due to a blockade of multiple Rydberg excitations [55]. Hence, the absorption contrast, $(\alpha_0 - \alpha)/\alpha$, between single-photon driving, $\alpha_0 = \alpha_{\mathrm{res}} + \alpha_{\mathrm{bg}}$, and two-photon excitation, α, provides a suitable figure of merit for estimating the extent of blockade effects on the optical response. As shown in Fig. 4, the contrast is maximal for $\Gamma_s = 0$ and around $\beta = 1$. Since the nondissipative dark state established under EIT conditions is perturbed by decoherence and decay of the Rydberg state, the contrast tends to decrease as the decay rate Γ_s increases. While precise values for Γ_s remain to be determined experimentally, one can expect comparable coherence properties as measured for p-state Rydberg excitons at cryogenic temperatures, suggesting that Γ_s is in the μeV range for high principal quantum numbers, $n \gtrsim 10$ [22]. This suggests that considerable blockade-induced absorption contrasts of $(\alpha_0 - \alpha)/\alpha \approx 3$ are feasible.

While resonant p-state coupling maximizes the achievable contrast for optimal values of β, it also implies a strong β dependence that originates from the interference between the two different excitation pathways, as discussed above. An interesting alternative approach is, therefore, to deliberately operate far off any p-state resonance and establish conditions of EIT only via the background. Consequently, this offers a robust way to establish dark exciton states in the material. As demonstrated in Fig. 1(c), the realization of such phonon-mediated EIT conditions indeed yields a spectrum of sharp transmission resonances for a dominant background path ($\beta > 1$), where the absorption drops to very small values whenever one hits a two-photon resonance with an excited Rydberg s state. EIT in this case is

indeed enabled predominantly by the continuum of phonon-dressed exciton states, since the probe laser is tuned right between the $2p$ and $3p$ resonances to render p-state excitation inefficient, i.e., $\beta \gg 1$. As a result, the absorption drops to a very small residual value at each transmission resonance, given by the Rydberg state linewidth, assumed $\Gamma_s = 5$ neV for the $1s$-para exciton and $0.8/n^3$ meV for the Rydberg states with $n > 1$. Here, we used the expected $\Omega \sim n^{-3/2}$ Rydberg-state scaling of the control Rabi frequency with a chosen prefactor $\Omega = 0.9/n^{3/2}$ meV.

As illustrated in Fig. 4, this phonon-mediated EIT also renders the absorption contrast much more insensitive to variations of β, since the Rydberg blockade can now switch solely between background-mediated EIT transmission and strong absorption via phonon-assisted exciton coupling. Thereby achievable absolute values of the absorption contrast are around $\alpha_0 - \alpha \sim 30$ mm^{-1}. This lies in the range of absorption coefficients that can be achieved in Rydberg-atom experiments with cold gases with densities around $\sim 10^{11}$ cm^{-3} [55]. Just like in the atomic case, the ability to realize EIT would offer a powerful approach to optically control and probe [56] the density of Rydberg excitons for experimental studies of strong interaction and blockade effects. For a typical blockade radius of about 5 μm [22], this corresponds to optical depths per blockade volume [57] of $\mathrm{OD}_b \approx 0.3$. These values are comparable to those obtained in magneto-optical traps for atomic gases [55] and would therefore already provide a platform for observing highly nonlinear light propagation with low-intensity coherent fields [55,58–60].

EIT can be implemented in various semiconductors that feature two long-lived exciton states. Cu_2O, for example, offers two viable approaches to realize the described scheme in experiments. On the one hand, two-photon coupling to the $1s$-para exciton of the yellow series via a low-lying p state, suggests excellent EIT conditions enabled by the extraordinarily small linewidth $\Gamma_s \sim 5$ neV of the $1s$ state [61,62]. This coupling scheme can be implemented with current laser technology and the narrow EIT resonances available in such a scenario would yield an approach to control phonon coupling. It may also be exploited to realize enhanced Kerr nonlinearities [63] and thereby generate strong effective interactions between dark-state polaritons. On the other hand, EIT can be realized via long-lived Rydberg s states excited in a two-photon ladder scheme. In this setup, the low-lying transition to a p-state exciton exhibits strong optical coupling, while the upper Rydberg-state transition can be driven with THz radiation [64].

In conclusion, we have presented a microscopic description of phonon-induced absorption processes in a semiconductor and showed how they can be controlled via exciton EIT. These findings are not limited to the presented example of Cu_2O, but generally apply to the broad class of semiconductors with indirect transitions to the exciton state, such as ZnO [65]. The developed approach to control phonon-mediated absorption in such materials provides a new spectroscopic tool to observe and probe the individual effects of exciton and phonon interactions in semiconductors. Moreover, the ability to suppress the phononic absorption background permits the realization of a series of narrow and isolated Rydberg lines, akin to Rydberg states in atomic gases. Following recent ideas and experiments in atomic Rydberg physics [13–21], this suggests new avenues to exploit the strong interactions between Rydberg excitons for nonlinear optics. The exploration of such ideas will require us to go beyond the single-exciton theory of this work, in order to understand the interplay of EIT and exciton-phonon coupling in the presence of multiple interacting excitons. Hereby, the possible integration into optical cavities presents another exciting outlook. In fact, already a moderate cavity enhancement of the probe-field coupling by a factor of ~ 10 would yield optical depths of $\mathrm{OD}_b \gtrsim 1$, and may therefore make it possible to generate photon correlations with Rydberg excitons.

The authors thank Richard Schmidt and Marc Aßmann for valuable discussions. This work has been supported by the EU through the H2020-FETOPEN Grant No. 800942640378 (ErBeStA), by the DFG through the SPP1929, by the Carlsberg Foundation through the Semper Ardens Research Project QCooL, by the DNRF through a Niels Bohr Professorship to T. P. and the DNRF Center of Excellence CCQ (Grant Agreement No. DNRF156), and by the NSF through a grant for the Institute for Theoretical Atomic, Molecular, and Optical Physics at Harvard University and the Smithsonian Astrophysical Observatory.

*valentin.walther@cfa.harvard.edu
†These authors contributed equally to this work.

[1] P. Schauß, M. Cheneau, M. Endres, T. Fukuhara, S. Hild, A. Omran, T. Pohl, C. Gross, S. Kuhr, and I. Bloch, Nature (London) **491**, 87 (2012).
[2] P. Schauß, J. Zeiher, T. Fukuhara, S. Hild, M. Cheneau, T. Macrì, T. Pohl, I. Bloch, and C. Gross, Science **347**, 1455 (2015).
[3] H. Labuhn, D. Barredo, S. Ravets, S. de Léséleuc, T. Macrì, T. Lahaye, and A. Browaeys, Nature (London) **534**, 667 (2016).
[4] J. Zeiher, R. van Bijnen, P. Schauß, S. Hild, J.-y. Choi, T. Pohl, I. Bloch, and C. Gross, Nat. Phys. **12**, 1095 (2016).
[5] J. Zeiher, J.-y. Choi, A. Rubio-Abadal, T. Pohl, R. van Bijnen, I. Bloch, and C. Gross, Phys. Rev. X **7**, 041063 (2017).
[6] H. Bernien, S. Schwartz, A. Keesling, H. Levine, A. Omran, H. Pichler, S. Choi, A. S. Zibrov, M. Endres, M. Greiner, V. Vuletić, and M. D. Lukin, Nature (London) **551**, 579 (2017).
[7] A. Keesling, A. Omran, H. Levine, H. Bernien, H. Pichler, S. Choi, R. Samajdar, S. Schwartz, P. Silvi, S. Sachdev, P. Zoller, M. Endres, M. Greiner, V. Vuletić, and M. D. Lukin, Nature (London) **568**, 207 (2019).

[8] S. de Léséleuc, V. Lienhard, P. Scholl, D. Barredo, S. Weber, N. Lang, H. P. Büchler, T. Lahaye, and A. Browaeys, Science **365**, 775 (2019).

[9] H. Levine, A. Keesling, G. Semeghini, A. Omran, T. T. Wang, S. Ebadi, H. Bernien, M. Greiner, V. Vuletić, H. Pichler, and M. D. Lukin, Phys. Rev. Lett. **123**, 170503 (2019).

[10] T. M. Graham, M. Kwon, B. Grinkemeyer, Z. Marra, X. Jiang, M. T. Lichtman, Y. Sun, M. Ebert, and M. Saffman, Phys. Rev. Lett. **123**, 230501 (2019).

[11] I. S. Madjarov, J. P. Covey, A. L. Shaw, J. Choi, A. Kale, A. Cooper, H. Pichler, V. Schkolnik, J. R. Williams, and M. Endres, Nat. Phys. **16**, 857 (2020).

[12] J. M. Raimond, M. Brune, and S. Haroche, Rev. Mod. Phys. **73**, 565 (2001).

[13] Y. O. Dudin and A. Kuzmich, Science **336**, 887 (2012).

[14] T. Peyronel, O. Firstenberg, Q.-Y. Liang, S. Hofferberth, A. V. Gorshkov, T. Pohl, M. D. Lukin, and V. Vuletic, Nature (London) **488**, 57 (2012).

[15] L. Li, Y. O. Dudin, and A. Kuzmich, Nature (London) **498**, 466 (2013).

[16] H. Gorniaczyk, C. Tresp, P. Bienias, A. Paris-Mandoki, W. Li, I. Mirgorodskiy, H. P. Büchler, I. Lesanovsky, and S. Hofferberth, Nat. Commun. **7**, 12480 (2016).

[17] J. D. Thompson, T. L. Nicholson, Q.-Y. Liang, S. H. Cantu, A. V. Venkatramani, S. Choi, I. A. Fedorov, D. Viscor, T. Pohl, M. D. Lukin, and V. Vuletić, Nature (London) **542**, 206 (2017).

[18] H. Busche, P. Huillery, S. W. Ball, T. Ilieva, M. P. A. Jones, and C. Adams, Nat. Phys. **13**, 655 (2017).

[19] A. Paris-Mandoki, C. Braun, J. Kumlin, C. Tresp, I. Mirgorodskiy, F. Christaller, H. P. Büchler, and S. Hofferberth, Phys. Rev. X **7**, 041010 (2017).

[20] C. Murray and T. Pohl, Adv. At. Mol. Opt. Phys. **65**, 321 (2016).

[21] O. Firstenberg, C. S. Adams, and S. Hofferberth, J. Phys. B **49**, 152003 (2016).

[22] T. Kazimiercuk, D. Fröhlich, H. Stolz, S. Scheel, and M. Bayer, Nature (London) **514**, 343 (2014).

[23] M. Aßmann, J. Thewes, D. Fröhlich, and M. Bayer, Nat. Mater. **15**, 741 (2016).

[24] F. Schweiner, J. Main, G. Wunner, M. Freitag, J. Heckötter, C. Uihlein, M. Aßmann, D. Fröhlich, and M. Bayer, Phys. Rev. B **95**, 035202 (2017).

[25] F. Schweiner, J. Laturner, J. Main, and G. Wunner, Phys. Rev. E **96**, 052217 (2017).

[26] F. Schweiner, J. Main, and G. Wunner, Phys. Rev. E **95**, 062205 (2017).

[27] S. Zielińska-Raczyńska, D. Ziemkiewicz, and G. Czajkowski, Phys. Rev. B **95**, 075204 (2017).

[28] P. Rommel, F. Schweiner, J. Main, J. Heckötter, M. Freitag, D. Fröhlich, K. Lehninger, M. Aßmann, and M. Bayer, Phys. Rev. B **98**, 085206 (2018).

[29] S. Zielińska-Raczyńska, D. A. Fishman, C. Faugeras, M. M. P. Potemski, P. H. M. van Loosdrecht, K. Karpiński, G. Czajkowski, and D. Ziemkiewicz, New J. Phys. **21**, 103012 (2019).

[30] J. Heckötter, M. Freitag, D. Fröhlich, M. Aßmann, M. Bayer, P. Grünwald, F. Schöne, D. Semkat, H. Stolz, and S. Scheel, Phys. Rev. Lett. **121**, 097401 (2018).

[31] J. Heckötter, D. Janas, R. Schwartz, M. Aßmann, and M. Bayer, Phys. Rev. B **101**, 235207 (2020).

[32] V. Walther and T. Pohl, Phys. Rev. Lett. **125**, 097401 (2020).

[33] S. O. Krüger, H. Stolz, and S. Scheel, Phys. Rev. B **101**, 235204 (2020).

[34] S. O. Krüger and S. Scheel, Phys. Rev. B **97**, 205208 (2018).

[35] S. Steinhauer, M. A. M. Versteegh, S. Gyger, A. W. Elshaari, B. Kunert, A. Mysyrowicz, and V. Zwiller, Commun. Mater. **1**, 11 (2020).

[36] V. Walther, S. O. Krüger, S. Scheel, and T. Pohl, Phys. Rev. B **98**, 165201 (2018).

[37] J. Heckötter, M. Freitag, D. Fröhlich, M. Aßmann, M. Bayer, M. A. Semina, and M. M. Glazov, Phys. Rev. B **96**, 125142 (2017).

[38] V. Walther, R. Johne, and T. Pohl, Nat. Commun. **9**, 1309 (2018).

[39] M. Khazali, K. Heshami, and C. Simon, J. Phys. B **50**, 215301 (2017).

[40] A. N. Poddubny and M. M. Glazov, Phys. Rev. Lett. **123**, 126801 (2019).

[41] R. J. Elliott, Phys. Rev. **108**, 1384 (1957).

[42] F. Schöne, H. Stolz, and N. Naka, Phys. Rev. B **96**, 115207 (2017).

[43] K.-J. Boller, A. Imamoğlu, and S. E. Harris, Phys. Rev. Lett. **66**, 2593 (1991).

[44] M. Fleischhauer, A. Imamoğlu, and J. P. Marangos, Rev. Mod. Phys. **77**, 633 (2005).

[45] M. Artoni, G. C. La Rocca, and F. Bassani, Europhys. Lett. **49**, 445 (2000).

[46] F. Bassani, G. L. Rocca, and M. Artoni, J. Lumin. **110**, 174 (2004).

[47] F. Schweiner, J. Main, and G. Wunner, Phys. Rev. B **93**, 085203 (2016).

[48] J. Thewes, J. Heckötter, T. Kazimierczuk, M. Aßmann, D. Fröhlich, M. Bayer, M. A. Semina, and M. M. Glazov, Phys. Rev. Lett. **115**, 027402 (2015).

[49] F. Schöne, S.-O. Krüger, P. Grünwald, H. Stolz, S. Scheel, M. Aßmann, J. Heckötter, J. Thewes, D. Fröhlich, and M. Bayer, Phys. Rev. B **93**, 075203 (2016).

[50] S. Zielińska-Raczyńska, G. Czajkowski, and D. Ziemkiewicz, Phys. Rev. B **93**, 075206 (2016).

[51] A. M. Konzelmann, S. O. Krüger, and H. Giessen, Phys. Rev. B **100**, 115308 (2019).

[52] See Supplemental Material at http://link.aps.org/supplemental/10.1103/PhysRevLett.125.173601 for details on the derivation of the dressed-state description, leading to Eqs. (4)–(6), the optical response of the background with finite Γ, Eq. (10), and the analysis of the different limiting cases of the susceptibility.

[53] P. Grünwald, M. Aßmann, J. Heckötter, D. Fröhlich, M. Bayer, H. Stolz, and S. Scheel, Phys. Rev. Lett. **117**, 133003 (2016).

[54] P. W. Baumeister, Phys. Rev. **121**, 359 (1961).

[55] J. D. Pritchard, D. Maxwell, A. Gauguet, K. J. Weatherill, M. P. A. Jones, and C. S. Adams, Phys. Rev. Lett. **105**, 193603 (2010).

[56] A. K. Mohapatra, T. R. Jackson, and C. S. Adams, Phys. Rev. Lett. **98**, 113003 (2007).

[57] A. V. Gorshkov, J. Otterbach, M. Fleischhauer, T. Pohl, and M. D. Lukin, Phys. Rev. Lett. **107**, 133602 (2011).

[58] S. Sevinçli, N. Henkel, C. Ates, and T. Pohl, Phys. Rev. Lett. **107**, 153001 (2011).
[59] J. Han, T. Vogt, and W. Li, Phys. Rev. A **94**, 043806 (2016).
[60] A. Tebben, C. Hainaut, V. Walther, Y. C. Zhang, G. Zürn, T. Pohl, and M. Weidemüller, Phys. Rev. A **100**, 063812 (2019).
[61] S. Koirala, N. Naka, and K. Tanaka, J. Lumin. **134**, 524 (2013).
[62] R. Schwartz, N. Naka, F. Kieseling, and H. Stolz, New J. Phys. **14**, 023054 (2012).
[63] H. Schmidt and A. Imamoglu, Opt. Lett. **21**, 1936 (1996).
[64] A. Pagies, G. Ducournau, and J.-F. Lampin, APL Photonics **1**, 031302 (2016).
[65] Ü. Özgür, Y. I. Alivov, C. Liu, A. Teke, M. A. Reshchikov, S. Doğan, V. Avrutin, S.-J. Cho, and H. Morkoç, J. Appl. Phys. **98**, 041301 (2005).